τ = shear stress at a point in the pipe, lb./sq. ft.
τ_o = shear stress at the pipe wall, lb./sq. ft.
μ = gas viscosity, lb./ft.-sec.

LITERATURE CITED

1. Albright, C. W., J. H. Holden, H. P. Simons, and L. D. Schmidt, *Ind. Eng. Chem.*, **43**, 1837–1840 (1951).
2. Belden, D. H., and L. S. Kassel, *ibid.*, **41**, 1174–1181 (1949).
3. Chin-Yung, Wen, and H. P. Simons, *A.I.Ch.E. J.*, **5**, 263 (1959).
4. Clark, R. H., D. E. Charles, J. F. Richardson, and D. M. Newitt, *Trans. Inst. Chem. Eng.*, **30**, 209 (1952).
5. Deissler, R. G., *Natl. Advisory Committee Aeronaut. Tech. Note No. 2138* (July, 1950).
6. Depew, C. A., Ph.D. thesis, Univ. California (1960).
7. Farber, L., *Ind. Eng. Chem.*, **41**, 1184-1191 (1949).
8. Gasterstadt, H., *Z. Ver Deut. Ing.*, **265**, 3-75 (1924).
9. Gill, W. N., and M. Scher, *A.I.Ch.E. J.*, **7**, 61-63 (1961).
10. Hariu, O. H., and M. C. Molstad, *Ind. Eng. Chem.*, **41**, 1148–1160 (1949).
11. Helander, R. E., Ph.D. thesis, Northwestern Univ., Evanston, Illinois (1956).
12. Hinkle, B. L., Ph.D. thesis, Georgia Inst. Technol., Atlanta, Georgia (1953).
13. Julian, F. M., M.S. thesis, Univ. Houston, Houston, Texas (1964).
14. Kada, H., and T. J. Hanratty, *A.I.Ch.E. J.*, **6**, 624 (1960).
15. Koble, R. A., Ph.D. thesis, Univ. West Virginia, Morgantown, West Virginia (1952).
16. Korn, A. H., *Chem. Eng.*, **57**, No. 3, 108-111 (1950).
17. Mehta, N. C., Ph.D. thesis, Purdue Univ., Lafayette, Indiana (1955).
18. Mitlin, L., Ph.D. thesis, Univ. London, London, England (1954).
19. Soo, S. L., *Ind. Eng. Chem. Fundamentals*, **1**, 33 (1962).
20. ———, *Chem. Eng. Sci.*, **9**, 57 (1956).
21. ———, H. K. Ihrig, and A. F. El Kouh, *J. Basic Eng.*, **82**, 609 (1960).
22. Soo, S. L., and C. L. Tien, *J. Appl. Mech.*, **27E**, 5 (1960).
23. Soo, S. L., G. J. Treyek, R. C. Dimick, and G. F. Hohnstreiter, *Ind. Eng. Chem. Fundamentals*, **3**, 98 (1964).
24. Torobin, L. B., and W. H. Gauvin, *Can. J. Chem. Eng.*, Parts I-III, **37** (1959); Parts IV, V, **38** (1960); Part VI, **39** (1961).
25. Vogt, E. G., and R. R. White, *Ind. Eng. Chem.*, **40**, 1731–1738 (1948).
26. Von Karman, T., *J. Aeronaut. Sci.*, **1**, 1-20 (1934).
27. Welschof, G., *VDI Forschungsheft*, **492**, 5 (1962).

Manuscript received November 20, 1964; revision received April 15, 1965; paper accepted April 29, 1965. Paper presented at A.I.Ch.E. San Francisco meeting.

Suction Nucleate Boiling of Water

P. C. WAYNER, JR., and A. S. KESTEN

United Aircraft Corporation Research Laboratories, East Hartford, Connecticut

Suction nucleate boiling (consisting of saturated pool boiling on a porous heat source with the generated vapor exhausting through the pores) was investigated experimentally and theoretically. The experimental results demonstrated that: (1) interfacial free energy can be used to direct the flow of liquid and vapor in a desired direction and to separate vapor from liquid at the point of vapor generation; (2) the heat transfer coefficient for suction nucleate boiling is higher than that associated with normal boiling; and (3) a porous heat exchanger can be designed to give stable transition from nucleate to film boiling. The theoretical analysis, which was based on experimental observations, indicated that extremely high heat fluxes and heat transfer coefficients are possible with small pores. Comparison of the experimental and theoretical results demonstrated that the full potential of suction nucleate boiling was not attained in the experiments and indicated some of the experimental refinements needed to attain this potential.

The feasibility and limitations of many engineering devices depend on normal boiling heat transfer. The results of extensive study in this field have demonstrated that normal boiling is an extremely complex phenomenon with many undesirable characteristics, such as random nucleation and fluid flow; an area of hydrodynamic instability; a heat transfer coefficient dependent on many variables including heat flux, vapor quality, and gravity; a low average heat flux and heat transfer coefficient in the film boiling regime or when a high quality product is desired; and difficulty in obtaining 100% quality vapor because of liquid entrainment. In an effort to eliminate some of these undesirable characteristics, a modified mode of heat transfer consisting of film boiling on a porous heat source with the generated vapor exhausting through the heat source has been proposed (*1*) and studied experimentally (*2*, *3*). The results of these film boiling studies demonstrated the feasibility and advantages of this concept. Since the heat transfer coefficient and heat flux are higher in nucleate boiling than in film boiling, a logical extension of the film boiling work is the study of nucleate boiling on a porous heat source with the generated vapor exhausting through the heat source. This mode of heat transfer, herein designated suction nucleate boiling (S.N.B.), has not been previously studied. The basic difference between suction nucleate boiling and film boiling on a porous heating ele-

P. C. Wayner, Jr., is with the Rensselaer Polytechnic Institute, Troy, New York.

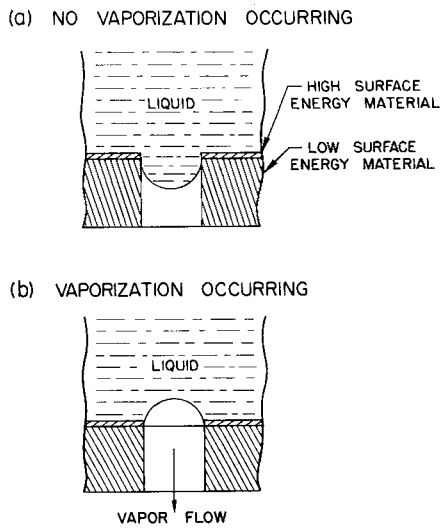

Fig. 1. Pore cross section.

ment is that the phase change occurs at the surface of the porous heating element in S.N.B., while the phase change occurs well away from the surface in film boiling. Depending on the porous heat transfer surface design and operating conditions, suction nucleate boiling offers the following possible advantage: (1) control of bubble nucleation, (2) elimination of the hydrodynamic resistance to vapor removal, (3) a large decrease in the effect of gravity on boiling, (4) an increase in the heat transfer coefficient over that of normal nucleate boiling, (5) extension of the nucleate boiling regime to higher heat fluxes, (6) stable transition into film boiling, and (7) generation of either a saturated or superheated vapor. The objective of the work described herein was to investigate both theoretically and experimentally the feasibility and inherent advantages of suction nucleate boiling.

DISCUSSION OF SNB CONCEPT

In general, suction nucleate boiling utilizes the forces derived from interfacial free energy to supply liquid to the evaporating interface, control bubble nucleation, separate vapor from liquid at the point of vapor generation, and direct the flow of vapor. Ideally, a porous heat source would be composed of a regular pattern of small, parallel, cylindrical pores designed to stabilize the menisci in a desired plane of evaporation. In this paper we are concerned with stabilizing the menisci at the outer surface of the pores in the porous heat source. Figure 1 is a cross-sectional drawing of a particular heat source design showing one of these pores and a portion of its zone of influence. The zone of influence of a pore is defined as that portion of the heat exchanger primarily influenced by that particular pore. In this design, the outer surface of the heat source is composed of a high surface energy material (for example, copper) to ensure "wetting" of the solid by the liquid (for example, water), and a portion of the surface of the pore is composed of a low surface energy material (for example, Teflon) to ensure "nonwetting" of that portion of the pore surface by the liquid. It should be noted that the lower the surface tension of the liquid, the lower the surface energy of the material required for the nonwetted portion of the pore surface. In Figure 1*a*, a pore is shown when there is no vaporization occurring, and a column of liquid is supported by surface tension acting through the obtuse contact angle between the liquid-vapor interface and the low energy surface. In Figure 1*b*, a pore is shown with vaporization (boiling) occurring. With the use of the concept of free surface energy, it has been shown that nucleation from a solid surface at a temperature near the saturation point is very improbable in ebullition unless a gas or vapor pocket is present to act as a nucleation site; therefore, in suction nucleate boiling vaporization occurs preferentially at the pores where vapor continuously exists. In this case, surface tension acting through an acute contact angle between the liquid-vapor interface and the high energy surface forces the vapor through the pore. Since the pressure difference across the liquid-vapor interface is proportional to the surface tension of the liquid and inversely proportional to the radius of curvature of the meniscus, substantial pressure differences are attainable with very small pores. The pressure difference across a hemispherical liquid-vapor interface of 1 μ radius in water is approximately 16 lb./sq. in. In order to maintain a high volumetric flow rate in small pores, it would be possible to apply an external pressure drop across the pore; the meniscus pressure drop, which varies with the radius of curvature, would control any fluctuations that occur in the evaporation rate. Removal of vapor through a large number of small nucleating pores eliminates the need for the large scale turbulence associated with normal boiling and results in an extremely short conduction path between the thermal energy source and point of vapor generation.

EXPERIMENTAL STUDIES

The experimental studies were designed to investigate the feasibility of suction nucleate boiling, determine the operating characteristics of a heat transfer element operating in the suction nucleate boiling regime, and suggest a theoretical model for analysis.

Test Apparatus

Since it would be difficult to construct a microporous surface using the pore design presented in Figure 1, it was found advantageous to make two modifications in the design of the heat transfer zone, taking advantage of both the substantial controlling forces associated with smaller pores and the simple construction of a regular pattern of relatively large pores. The first modification was to place an additional nonheatgenerating porous element of a relatively high free surface energy material (Alundum) with smaller pores in contact with the liquid side of the porous heat-generating element. A cross-sectional drawing of such a configuration (designated experimental design "*A*") is presented in Figure 2. Because the pressure differential due to surface tension is inversely proportional to

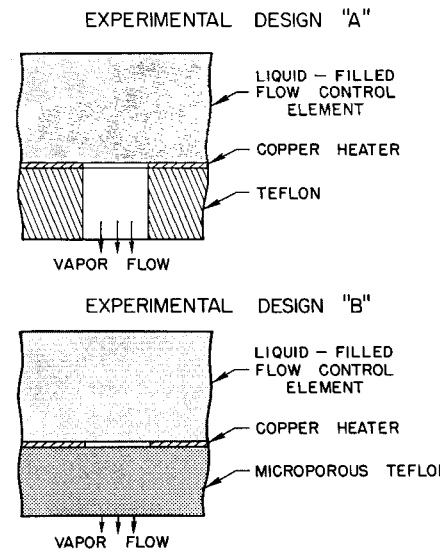

Fig. 2. Cross section of experimental designs "A" and "B."

the radius of the pore, the smaller pore radius in the additional porous element greatly magnifies the pressure available for directing the flow of vapor through the pores of the heat-generating element. Since this additional porous element has a higher thermal conductivity than water, it also enhances heat conduction from the solid portion of the heat-generating element to the liquid-vapor interface. The feasibility of this type of flow control element has been previously demonstrated in film boiling with vapor suction (2, 3). The second modification was to replace the cylindrical pore through the Teflon by microporous Teflon which increased the resistance to liquid flow in the exhaust direction and, therefore, is a liquid-vapor separator. This configuration (designated experimental design "*B*") is also depicted in Figure 2. Experiments were performed with each of these configurations.

A cross-sectional drawing of the general configuration of the experimental heat transfer cell is presented in Figure 3. The construction using pore design "*A*" will be described first. The heat transfer surface was made from a circular, 5.5 in. diameter, copper-clad, Teflon plate composed of 0.0014 in. thick copper laminated to 0.015 in. thick Teflon (Raybestos-Manhattan, Inc., No. 100-1). Except for a 1-in. strip of copper across the middle of this plate, the copper cladding was removed by chemical etching. The copper strip was used as a d.c. resistance heater. Copper was selected for use in this application in order to avoid hot spots which would act as extraneous nucleation sites on the heat transfer surface. The middle 1 × 1 in. portion of this copper-clad Teflon strip was made porous by drilling 0.010 in. diameter holes in a hexagonal pattern. The number and spacing of the holes for the various experiments are indicated in Table 1. The etched, copper-clad Teflon plate was supported by a 0.75 in. thick, ceramic filled, Teflon plate (Polymer Corporation Fluorosint) and clamped between two 3.5 in. I.D. Pyrex pipes which acted as a saturated water reservoir and a flow channel for the generated vapor, respectively. A path for the vapor flow through the support plate was made by inserting a 1.1 × 1.1 × 0.75 in. porous support plate (fused refractory with a pore diameter of approximately 100μ) directly under the drilled pores in the heat transfer element. The flow control element was a 1 × 1 × 0.187 in. porous Alundum plate (Norton No. RA 360 clay bonded alumina) which had an apparent porosity of 29% and a particle retention in filtration of 5μ. Auxiliary heaters were located around the heat transfer area to minimize heat losses from the vapor channel and to maintain the boiling liquid in the reservoir at saturation. In order to permit collection of the generated vapor and thereby permit measurement of its flow rate, a condenser was attached to the exhaust channel. Copper-constantan thermocouples were used to measure temperature at various locations in the heat transfer zone.

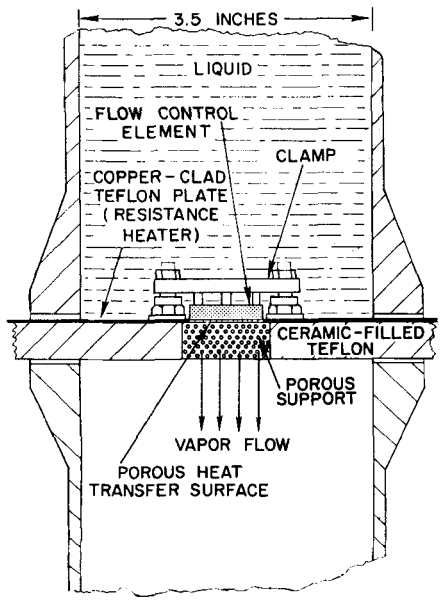

Fig. 3. Cross section of experimental heat transfer cell.

Table 1. Dimensions and Heat Transfer Coefficients for Experimental Designs "*A*" and "*B*"

Experimental design	*A*	*A*	*B*
Pore density, pores/sq. in.	1150	1755	1090
a, ft. × 10^4	4.17	4.17	6.67
b, ft. × 10^3	1.30	1.07	1.47
h_{ea}, B.t.u./(hr.)(sq. ft.)(°F.) × 10^{-4}	1.06	2.30	0.45
h_{ta}, (Model "*A*"), B.t.u./(hr.)(sq. ft.)(°F.) × 10^{-4}	4.44	8.50	—
h_{ta}, (Model "*B*"), B.t.u./(hr.)(sq. ft.)(°F.) × 10^{-4}	0.87	1.24	0.86
h_{ep}, B.t.u./(hr.)(sq. ft.)(°F.) × 10^{-5}	2.09	2.98	—
h_{tp}, (Model "*A*"), B.t.u./(hr.)(sq. ft.)(°F.) × 10^{-5}	8.77	11.0	—
h_{ep}/h_{tp}, %	23.8	27.1	—

The experimental heat transfer cell for the study of pore design "*B*" was constructed by making the following changes in the above test apparatus. In this design the resistance heater was made from a 1 × 5.5 in. strip of copper, 0.0014 in. thick, with a hexagonal pattern of punched 0.016 in. diameter holes. The spacing and the number of holes are given in Table 1. Instead of the Teflon backing, which was laminated to the copper used in pore design "*A*" a circular, 5.5 in. diameter, 0.063 in. thick, microporous, Teflon plate (Pall Corporation porous Teflon) with a mean pore diameter of 9μ was placed under the copper strip to provide support. The middle 1 × 1.19 in. of the porous copper were covered with a 1.19 × 1.19 × 0.187 in. porous Alundum plate (Norton No. RA 84) which had an apparent porosity of 33.5% and a particle retention in filtration of 0.1μ. Thus, that portion of the porous copper resistance heater in suction nucleate boiling was sandwiched between microporous Alundum and microporous Teflon. The dimensions of the porous support plate were 1.3 × 1.3 × 0.75 in. In order to permit operation with high values of pressure drop across the heat transfer element, the heat transfer cell was fitted with a sealed water supply reservoir and pressure gauge. The d.c. power input to the resistance heater was supplied by a Rapid Electric, Model 3006, 3,000 amp., 6 v., stabilized silicon rectifier. The voltage across the electrically heated surface and the electromotive forces of the thermocouples were measured with a K-3 Leeds and Northrup potentiometer. The heating current was measured with a calibrated Weston Model 273 d.c. ammeter in conjunction with a constant resistance shunt placed in series with the resistance heater.

Operating Procedure

In all the experiments the heat transfer cell was filled with boiling, deionized water to a prescribed depth which was maintained constant during cell operation; the exhaust channel was vented to the atmosphere; and the water was kept at the saturation point with auxiliary heaters which were also used to minimize heat losses from the heat transfer zone. For the higher pressure drop experiments, the heat transfer cell was operated above atmospheric pressure by sealing the saturated water reservoir and allowing the vapor pressure to increase to the desired value. For each test the power input was set at the level of interest and 20 min. were allowed for the equipment to reach steady state before measurements were taken. Measurements were made of the voltage drop across the porous surface and the constant resistance shunt, the current, the pressure head, and the temperatures at various locations in the heat transfer cell. The average temperature of the heat transfer surface was obtained by measuring the change in its electrical resistance from that at a known base temperature. The voltage drops across the shunt and the unknown resistance of the resistance heater were measured with the potentiometer at a base temperature and during operation. The base temperature was measured with a potentiometer and

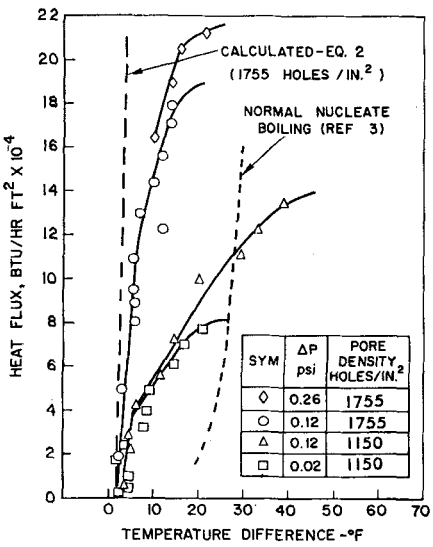

Fig. 4. Heat flux vs. temperature difference for experimental design "A."

calibrated thermocouple. These measurements were sufficient to determine the unknown temperature. The flow through the porous plate was condensed and measured for a period of 15 to 20 min. It was not possible to measure the temperature of the exhaust as it left the porous heat transfer surface, because auxiliary heaters were used to prevent condensation due to heat losses in the exhaust channel. However, since the vapor left the heat transfer zone at saturation when the heat transfer cell operated in the nucleate boiling regime, this was not an obstacle to the calculation of a heat balance. The auxiliary heaters did not supply sufficient heat to the evaporating interface to interfere with the determination of a heat balance because the temperature below the Teflon was maintained at approximately the saturation temperature.

Data Reduction and Error Estimation

For experimental design "*B*" the heat flux was taken equal to the heat of vaporization of the condensate collected per unit of time and area assuming that the vapor left the porous plate at the average plate temperature. This heat flux agreed to within ±7% of that calculated using the voltage and current measurements when the average porous plate temperature was equal to that of the electrical contacts leading to the porous plate. When these two temperatures differed, the difference in the calculated fluxes was taken equal to the heat loss or gain by conduction in the electrical contacts. The superficial area of the porous heat transfer surface, that is, the projected area of copper and pores perpendicular to the fluid flow direction, was used in these calculations. For experimental design "*A*" the heat flux was taken equal to the power input corrected for the heat gained by conduction in the electrical contacts. The magnitude of the required correction was estimated from the data of experimental design "*B*." The other heat calculation errors were assumed negligible, since the auxiliary heaters maintained the surrounding zone at the saturation temperature. It was not possible to use the condensate for heat flux calculations in experimental design "*A*" because of liquid entrainment in the vapor exhaust, which is discussed below. The maximum relative error in the heat flux calculation using the electrical measurements was ±6% which resulted from a ±3% error in the area, a ±1% error in the voltage measurement, and a ±2% error in the current measurement. These calculated fluxes agreed with the fluxes based on the condensate measurements when the electrical contacts were at the same temperature as the porous plate; therefore, a heat balance was established with these error limits. The estimated maximum error in the temperature of the porous heat transfer surface is ±4°F.

Experimental Results

In Figure 4 the experimentally determined heat flux based on the superficial area is plotted vs. average temperature difference between the copper and evaporating interface for the suction nucleate boiling of saturated water using experimental design "*A*." The effects of pore density and pressure drop are shown. These pressure drops occurred between the top of the flow control element and the bottom of the porous support. In these experiments all the vapor flowed in a direction contrary to that of normal buoyancy. For reference, previously published data for the nucleate boiling of water on a 4/0 polished copper surface are also shown (*4*). The data demonstrate that: (1) the heat transfer coefficient for suction nucleate boiling is substantially higher than that associated with normal boiling; (2) surface tension can be used to direct the flow of vapor in a desired direction; and (3) an increase in pore density and/or pressure drop gives higher heat fluxes and an increase in the heat transfer coefficient. A small increase in heat flux above the last experimental point in the individual curves resulted in a slow drift toward much higher surface temperatures and in vapor flowing from the top of the flow control element. This last point is designated departure from nucleate boiling and corresponds to departure from nucleate boiling in normal boiling. It should be noted that the total internal surface areas of the pores in the metal for the two configurations are 0.05 sq. in. for the 1,150 pores and 0.077 sq. in. for the 1,755 pores, and that departure from nucleate boiling at the same pressure drop occurs at a correspondingly higher flux with additional pore surface. The individual curves have a characteristic shape of two straight lines of different slope. The initial slope is considered the region of nucleate boiling. The second portion of the curve may be considered a transition region between nucleate boiling and film boiling. It was also found that liquid was entrained in the vapor exhaust. The volume of entrained liquid ranged from 40% of the condensed liquid-vapor volume at higher fluxes to 90% at lower fluxes. This entrainment was eliminated by the use of experimental design "*B*."

In Figure 5 the experimentally determined heat flux based on the superficial area obtained using experimental design "*B*" is plotted vs. the average temperature difference for various pressure drops. These pressure drops occurred between the top of the flow control element and the bottom of the porous support. In these experiments surface tension was used to direct the flow of all the vapor in a direction contrary to that of normal buoyancy and to separate vapor from liquid at the point

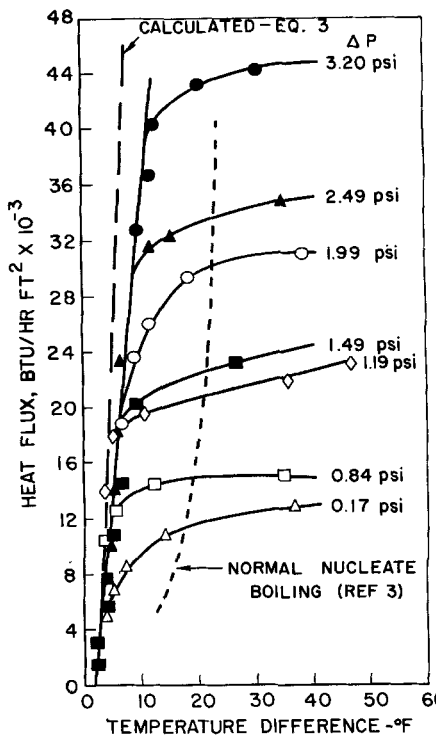

Fig. 5. Heat flux vs. temperature difference for experimental design "B."

of generation. The calculations described above indicated that the exhaust quality was 100%. The individual curves have the characteristic shape of an initial straight line, which is considered the nucleate boiling region, followed by a smooth transition into film boiling. Unlike experimental design "A," no vapor was observed coming from the top of the flow control element in any of the experiments. The data demonstrate that: (1) while operating in the nucleate boiling regime, the measured heat transfer coefficient for suction nucleate boiling is substantially higher than that associated with normal boiling; (2) the point of departure from nucleate boiling is a function of pressure drop; (3) the transition from nucleate to film boiling is stable; and (4) it is possible to use surface tension to separate vapor from liquid and to direct the flow of vapor in a desired direction. Due to the limited scope of the experiments, the effect of higher heat fluxes was not investigated. Though not measured, it is anticipated that higher fluxes are attainable with these pore dimensions at higher pressure drops.

Results have been published that demonstrated the use of nonwetted nucleation sites to obtain high heat transfer coefficients in normal nucleate boiling (*5, 6*), and the use of wicking material on a solid heat transfer surface (*7* to *9*). Although these papers are related to the present paper under the general concept of the use of interfacial free energy to control the boiling process, a discussion concerning this general concept is omitted because of the particular nature and length of this paper.

ANALYTICAL STUDIES

Proposed Mechanism

Based on the experimental data and observations discussed previously, a hypothetical heat transfer mechanism is proposed for each experimental design and is used in a theoretical analysis of the suction nucleate boiling process. As regards experimental design "A," the low surface temperature, the pore design itself, and the entrainment of liquid in the generated vapor indicated that some liquid was always present in that portion of the pore surrounded by metal and that vaporization occurred at the copper wall of the pore. The flow control element prevented the generated vapor from flowing up into the bulk liquid; the generated vapor with entrained liquid exhausted through the Teflon. (It should be noted that the pressure drop across a meniscus with a radius of curvature equal to the radius of the copper pore is not sufficient to direct the flow of vapor downward.) Departure from nucleate boiling occurred in these pores when substantial resistance to vapor removal caused the liquid-vapor interface to move up into the flow control element. As regards experimental design "B," the slightly higher surface temperature, the absence of entrained liquid in the exhaust, the resistance to vapor removal, and the presence of a microporous Teflon surface penetrating up into a portion of the pore that was only 0.0014 in. long indicated that vapor predominated in the pore. The low free surface energy of the Teflon ensured that any vapor present readily coated its surface. It is proposed that in this case vaporization occurred at the boundary between the microporous Alundum and the pore. The flow control element prevented the vapor from going upward and the microporous Teflon prevented any eddies of liquid from passing downward. Departure from nucleate boiling occurred in this design also when substantial resistance to vapor removal caused the liquid-vapor interface to move up into the flow control element.

Analysis

A single pore in the copper heat generating element and its zone of influence in the porous Alundum are analyzed for experimental designs "A" and "B." The objective of the analysis was to determine the steady state

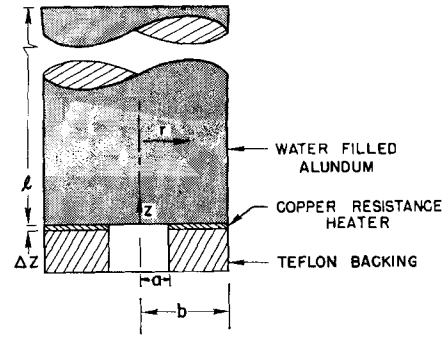

Fig. 6. Cross section of analytical model showing a single pore and pore zone of influence.

temperature distribution in the copper and in the water-filled Alundum as a function of position and heat flux. Although the pores in the experimental design were drilled in a hexagonal pattern, it was assumed that the temperature is symmetrical about the axis of the cylindrical pore. Since the area of the inscribed circle of a hexagon is equal to 91% of the area of the hexagon, and the temperature variation in the remaining portion of the hexagon was small, the assumption that the temperature profile exhibited cylindrical symmetry is a good one. Schematic diagrams of experimental designs "A" and "B" are shown in Figure 2 and a cross-sectional diagram of the analytical model is shown in Figure 6. In experimental design "A" it was presumed that heat was transferred from the copper heating element axially, to the water-filled Alundum contacting the upper surface of the copper, and radially to water contacting the inside surface of the pore. In experimental design "B" the presence of microporous Teflon below the pore was assumed to restrict radial heat transfer by retarding liquid entrainment within the pore. In both designs heat was assumed to be transferred by conduction in the water-filled Alundum.

The equations describing the temperature fields associated with experimental designs "A" and "B" are derived in the Appendix. For both designs the temperature in the water-filled Alundum is given by

$$T_w(r,z) = \frac{2}{b^2}\sum_{n=1}^{\infty}\frac{J_o(\alpha_n r)}{J_o^2(\alpha_n b)}\left[\frac{\cosh\alpha_n(l-z)}{\cosh\alpha_n l}\right]\int_o^b rT_o(r)\,J_o(\alpha_n r)dr \qquad (1)$$

In experimental design "A" the temperature distribution in the copper heating element was found to be

$$T_c(r) = \frac{S}{4}\left(a^2 - r^2 + 2b^2\ln\frac{r}{a}\right) + \frac{2\,S\,aH}{b^2}\sum_{n=1}^{\infty}\frac{J_1(\alpha_n a)}{\alpha_n^4 J_o^2(\alpha_n b)}\left[J_o(\alpha_n r) - J_o(\alpha_n a)\right] \qquad (2)$$

In experimental design "B" a discontinuity in temperature was assumed between the copper heating element and the vapor filling the pore. The temperature in the copper was then taken as uniform (see Appendix) and was found to be

$$T_c = \frac{S\,b^2(b^2-a^2)}{4\,H\,a^2\sum_{n=1}^{\infty}\frac{1}{\alpha_n}\left[\frac{J_1(\alpha_n a)}{J_o(\alpha_n b)}\right]^2} \qquad (3)$$

The average value of the theoretical heat transfer coefficient for experimental design "A" was obtained by integrating Equation (2) from $r = a$ to $r = b$ and by

evaluating the result for the design dimensions of interest. The average value of the theoretical heat transfer coefficient for experimental design "*B*" was obtained directly from Equation (3) by evaluating it for the design dimensions of interest. The calculated values of the theoretical coefficients based on the superficial area are presented in Table 1. The theoretical heat flux is plotted vs. temperature difference in Figures 4 and 5. In the calculations, the thermal conductivities of water-filled Alundum RA-84 and RA-360 were estimated to be 1.10 and 1.16 B.t.u./(hr.)(ft.)(°F.), respectively. The values for air-filled Alundum were obtained from Norton (*10*) and were adjusted for the presence of water with the method of Gorring and Churchill (*11*).

COMPARISON OF EXPERIMENTAL AND THEORETICAL RESULTS

Comparison of the experimental and theoretical results given in Table 1 shows that the theoretical model predicts higher heat transfer coefficients than were attained experimentally. The experimental results indicate the presence of an additional resistance to heat transfer which was not included in the theoretical model. In experimental design "*A*," where vaporization occurred primarily at the inside surface of the pore, this difference may be due to a thermal resistance at this surface which is not included in the idealized model. This resistance may represent incomplete contact between the liquid and surface. The ratio of the measured to the theoretical heat transfer coefficient, which may be taken as a measure of the degree of contact, was calculated for both pore densities, and the values are in agreement at around 25.5% (23.8% and 27.1%). In the transition region between nucleate boiling and departure from nucleate boiling, individual pores are believed to dry out with the liquid-vapor interface stabilizing at the surface of the flow control element. By taking the heat transferred per pore at the start of the transition region and dividing it by the theoretical heat transfer coefficient, one shows that this process is initiated at approximately the same temperature difference for both pore densities. Departure from nucleate boiling occurs when the vapor-liquid interface moves up into the flow control element. Referring to experimental design "*B*," the difference between the theoretical and experimental values is believed due to a thermal contact resistance between the heat source and flow control element which was neglected in the idealized model. Since the Alundum flow control element, which was pressed lightly against the copper, has a rough surface, this resistance might result from a thin layer of vapor surrounding the points at which the Alundum is in contact with the copper. The hypothesis that the surface layer of the flow control element is composed of vapor and Alundum is consistent with the assumption that the exhaust pores in this design were filled with vapor. Departure from nucleate boiling occurs, then, when the vapor-liquid interface moves up into the flow control element.

CONCLUDING REMARKS

The concept of suction nucleate boiling was investigated experimentally and theoretically. The experimental results demonstrated that: (1) interfacial free energy can be used to direct the flow of liquid and vapor in a desired direction and to separate vapor from liquid at the point of vapor generation; (2) the heat transfer coefficient for suction nucleate boiling is higher than that associated with normal boiling; and (3) a porous surface can be designed to give stable transition from nucleate boiling into film boiling. The theoretical analysis indicated that extremely high heat fluxes and heat transfer coefficients are possible with small pores. Comparison of the experimental and theoretical results demonstrated that the full potential of suction nucleate boiling was not attained in the experiments and indicated some of the experimental refinements needed to attain this potential (for example, minimizing the contact resistance in experimental design "*B*;" eliminating the liquid entrainment in experimental design "*A*;" and developing a heat exchanger with very small, parallel, cylindrical pores designed to stabilize the menisci at a desired plane of evaporation).

ACKNOWLEDGMENT

This research was undertaken as part of the United Aircraft Corporation Research Laboratories' corporate-sponsored program. The authors acknowledge the helpful discussions with and suggestions from Messrs. A. W. Blackman and J. R. Keilbach.

NOTATION

A_c = internal heat generation, B.t.u./(hr.)(cu.ft.)
A_n = constant defined by Equation (A-7)
a = pore radius, ft.
b = zone of influence radius, ft.
H = equal to $\dfrac{k_w}{\Delta z k_c}$
h = heat transfer coefficient, B.t.u./(hr.)(sq.ft.)(°F.)
k = thermal conductivity, B.t.u./(hr.)(ft.)(°F.)
l = thickness of flow control element, ft.
P = pressure, lb./sq.in.
q = heat flux, B.t.u./hr. sq.ft.
r = radial distance, ft.
S = equal to $\dfrac{A_c}{k_c}$
t = temperature, °F.
T = temperature minus liquid saturation temperature, °F.
z = vertical distance, ft.
Δz = copper thickness, ft.
α_n = roots of $J_o'(\alpha b) = 0$

Subscripts

c = copper
ta = theoretical value based on superficial area
tp = theoretical value based on the surface area of the copper portion of the pore
ea = experimental value based on superficial area
ep = experimental value based on the surface area of the copper portion of the pore
r = radial direction
s = saturation
w = water-filled Alundum

LITERATURE CITED

1. Bankoff, S. G., *Trans. Am. Soc. Mech. Engrs.*, **79**, 735 (1957).
2. Wayner, P. C., Jr., and S. G. Bankoff, *A.I.Ch.E. J.*, **11**, 59 (1965).
3. Pai, V. K., and S. G. Bankoff, *ibid.*, **11**, 65 (1965).
4. Gaertner, R. F., *Paper No. 63-WA-76*, Am. Soc. Mech. Engrs. Meeting, Philadelphia, Pa. (1963).
5. Young, R. K., and R. L. Hummel, *Chem. Eng. Progr.*, **60**, No. 7, 53 (1964).
6. Gaertner, R. F., discussion presented at Seventh Natl. Heat Transfer Conference, Cleveland, Ohio (August, 1964).
7. Allingham, W. D., and J. A. McEntire, *Trans. Am. Soc. Mech. Engrs. Ser. C*, **83**, 71 (1961).
8. Costello, C. P., and E. R. Redeker, *Chem. Eng. Progr. Symposium Ser. No. 41*, **59**, 104 (1963).

9. Costello, C. P., and W. J. Frea, *A.I.Ch.E. J.*, **10**, 393 (1964).
10. Bart, R. K., private communication, Norton Company, Worcester, Mass.
11. Gorring, R. L., and S. W. Churchill, *Chem. Eng. Progr.*, **57**, No. 7, 53 (1961).
12. Carslaw, H. S., and J. C. Jaeger, "Conduction of Heat in Solids," 2 ed., p. 219, Oxford Univ. Press, London, England (1959).
13. Irving, J., and N. Mullineux, "Mathematics in Physics and Engineering," 1 ed., p. 731, Academic Press, New York (1959).

APPENDIX A: DERIVATION OF EQUATIONS FOR TEMPERATURE FIELDS ASSOCIATED WITH PORE DESIGNS "A" AND "B"

The differential equation describing the temperature field in the water-filled alundum is

$$\frac{\partial^2 T_w}{\partial r^2} + \frac{1}{r}\frac{\partial T_w}{\partial r} + \frac{\partial^2 T_w}{\partial z^2} = 0 \qquad \begin{matrix} 0 \le r < b \\ 0 < z < l \\ T_w = (t_w - t_s) \end{matrix} \qquad \text{(A-1)}$$

The solution to this equation, subject to the boundary conditions of zero heat flux at $r = b$ and at $z = l$, is given by Carslaw and Jaeger (*12*) as

$$T_w = \sum_{n=1}^{\infty} A_n J_o(\alpha_n r)\left[\frac{\cosh \alpha_n (1 - z)}{\cosh \alpha_n l}\right] \qquad \text{(A-2)}$$

where

$$A_n = \frac{2}{b^2 J_o^2(\alpha_n b)} \int_o^b r f(r)\, J_o(\alpha_n r) dr \qquad \text{(A-3)}$$

and α_n, $n = 1, 2 \ldots$ are given by the positive roots of the equation

$$J_o'(\alpha b) = 0 \qquad \text{(A-4)}$$

The temperature distribution at $z = 0$, $f(r)$ will be determined below by the simultaneous solution of Equation (A-1) and the differential equation describing the temperature distribution in the copper resistance heater.

The hollow, cylindrical, copper element is a thin, uniform heat source insulated on the bottom side. The location of the copper resistance heater is shown in Figure 6. The differential equation describing the temperature distribution in the copper can be derived by making a heat balance over a cylindrical shell of infinitesimal thickness δr. It is assumed in the derivation that the copper element is so thin that the temperature at any radial position is constant across its width Δz. This assumption is justified by the high thermal conductivity of the copper and by the thinness of the copper. The heat balance over the cylindrical shell is

$$2\pi r \Delta z q_r|_r - 2\pi(r + \delta r)\Delta z q_r|_{r+\delta r} - \pi[(r + \delta r)^2 - r^2] q_z + \pi \Delta z[(r + \delta r)^2 - r^2] A_c = 0 \qquad \text{(A-5)}$$

Neglecting terms involving δr^2, rearranging, and letting $\delta r \to 0$ gives

$$\frac{q_z}{\Delta z} = -\frac{dq_r}{dr} - \frac{q_r}{r} + A_c \qquad \text{(A-6)}$$

Using

$$q_r = -k_c \frac{dT_c}{dr} \qquad \text{(A-7)}$$

and

$$q_z = -k_w \left.\frac{\partial T_w}{\partial z}\right|_{z=0} \qquad \text{(A-8)}$$

the resulting differential equation for the temperature distribution in the copper is

$$\frac{d^2 T_c}{dr^2} + \frac{1}{r}\frac{dT_c}{dr} = -S - H \left.\frac{\partial T_w}{\partial z}\right|_{z=0} \qquad \begin{matrix} a < r < b \\ z = 0 \\ T_c = (t_c - t_s) \end{matrix} \qquad \text{(A-9)}$$

where $S = \dfrac{A_c}{k_c}$ and $H = \dfrac{k_w}{\Delta Z k_c}$

Experimental Design "A"

Equation (A-9) can be solved together with the boundary conditions appropriate to experimental design "A."

$$\text{B.C. 1} \qquad \frac{dT_c}{dr} = 0 \qquad r = b \qquad \text{(A-10)}$$

$$\text{B.C. 2} \qquad T_c = 0 \qquad r = a \qquad \text{(A-11)}$$

The solution of Equation (A-9) is obtained by converting it into a Fredholm integral equation (*13*), which is

$$T_c(r) = \int_a^r \xi \ln \frac{\xi}{a}\left[S + H \left.\frac{\partial T_w(\xi)}{\partial z}\right|_{z=0}\right] d\xi + \ln \frac{r}{a}\int_r^b \xi \left[S + H \left.\frac{\partial T_w(\xi)}{\partial z}\right|_{z=0}\right] d\xi \qquad \text{(A-12)}$$

This equation can be solved implicitly for $T_c(r)$ by differentiating Equation (A-2) with respect to z, evaluating the result at $z = 0$, and substituting it into Equation (A-12) to get

$$T_c(r) = \frac{S}{4}(a^2 - r^2 + 2b^2 \ln \frac{r}{a}) - H \sum_{n=1}^{\infty} \frac{\tanh \alpha_n l\, A_n}{\alpha_n}[J_o(\alpha_n r) - J_o(\alpha_n a)] \qquad \text{(A-13)}$$

where

$$A_n = \frac{2}{b^2 J_o^2(\alpha_n b)} \int_a^b r\, T_c(r)\, J_o(\alpha_n r) dr \qquad \text{(A-14)}$$

assuming the temperature in the pore is the saturation temperature (that is, $f(r) = T_w(r, 0) = 0$ in the region $0 \le r < a$).

In order to get an explicit solution for $T_c(r)$, it remains now to obtain an expression for A_n which can be evaluated without knowing $T_c(r)$. Since $T_w(r, 0) = T_c(r)$ in the region $a < r < b$, Equation (A-9) can be subtracted from Equation (A-1) to get

$$\frac{\partial^2 T_w}{\partial z^2} - H \frac{\partial T_w}{\partial z} - S = 0 \quad z = 0, \quad a < r < b \qquad \text{(A-15)}$$

This equation can be generalized over the entire interval $0 \le r < b$ by writing it in the form

$$\frac{\partial^2 T_w}{\partial z^2} - H \frac{\partial T_w}{\partial z} - G(r) = 0 \quad z = 0 \quad G(r) = \begin{cases} g(r), & 0 \le r < a \\ S, & a < r < b \end{cases} \qquad \text{(A-16)}$$

The derivatives in Equation (A-16) can be evaluated at $z = 0$ in terms of A_n using Equation (A-2) to get

$$\sum_{n=1}^{\infty} \alpha_n^2 A_n J_o(\alpha_n r) + H \sum_{n=1}^{\infty} \alpha_n A_n \tanh \alpha_n l\, J_o(\alpha_n r) = G(r) \qquad \text{(A-17)}$$

This equation can be solved for A_n by using the fact that the Bessel functions are orthogonal over the interval $0 \le r < b$. Multiplying both sides of Equation (A-17) by $r\, J_o(\alpha_j r)$ and integrating between $r = 0$ and $r = b$ we have

$$A_n = \frac{\int_o^a r\, g(r)\, J_o(\alpha_n r)\, dr - \dfrac{Sa}{\alpha_n} J_1(\alpha_n a)}{\alpha_n(\alpha_n + H \tanh \alpha_n l)\dfrac{b^2}{2} J_o(\alpha_n b)} \qquad \text{(A-18)}$$

In order to determine $g(r)$ let us evaluate the derivatives in Equation (A-16) at $z = 0$ and in the interval $0 \le r < a$. $\dfrac{\partial^2 T_w}{\partial z^2}(r, 0)$ can be evaluated using Equation (A-1) and recalling that $T_w(r, 0)$ is taken as identically zero in the interval

$0 = r < a$ for experimental design "A." The derivatives $\frac{\partial T_w}{\partial r}$ and $\frac{\partial^2 T_w}{\partial r^2}$ must, therefore, approach zero as z approaches zero in this interval; consequently, $\frac{\partial^2 T_w}{\partial z^2}$ must also approach zero. A heat balance around the entire heat transfer zone can be used to evaluate the other derivative in Equation (A-16), $\frac{\partial T_w}{\partial z}(r, 0)$. Equating the total heat generated by the copper to the heat leaving the system radially at $r = a$ and axially at $z = 0$, we have

$$\pi \Delta z A_c (b^2 - a^2) = 2\pi k_w \int_0^a r \frac{\partial T_w}{\partial z}(r, 0) dr + 2\pi a \Delta z k_c \frac{dT_c}{dr}(a) \qquad \text{(A-19)}$$

Noting that we must specify the flux distribution as well as the temperature distribution between 0 and a to completely define the problem, $\frac{\partial T_w}{\partial z}(r, 0)$ is taken as constant in the interval $0 \leq r < a$. Equation (A-19) can now be solved for $\frac{\partial T_w}{\partial z}(r, 0)$ to get

$$\frac{\partial T_w}{\partial z}(r, 0) = \frac{S}{Ha^2}(b^2 - a^2) - \frac{2}{Ha}\frac{dT_c}{dr}(a) \quad 0 \leq r < a \qquad \text{(A-20)}$$

In the interval $0 \leq r < a$, Equation (A-16) can now be written as

$$g(r) = -H\frac{\partial T_w}{\partial z}(r, 0) = \frac{2}{a}\frac{dT_c}{dr}(a) - \frac{S}{a^2}(b^2 - a^2) \qquad \text{(A-21)}$$

$$0 \leq r < a$$

Substituting Equation (A-21) into Equation (A-18) and carrying out the required integration, we get

$$A_n = \frac{2 J_1(\alpha_n a)\left[2\frac{dT_c}{dr}(a) - \frac{Sb^2}{a}\right]}{\alpha_n^2(\alpha_n + H \tanh \alpha_n l)\, b^2 J_0^2(\alpha_n b)} \qquad \text{(A-22)}$$

In order to obtain an expression for $\frac{dT_c}{dr}(a)$, Equation (A-13), together with Equation (A-22), can be used to get

$$\frac{dT_c}{dr}(a) = \frac{\frac{S}{2a}\left[b^2 - a^2 - 4H\sum_{n=1}^{\infty}\frac{J_1^2(\alpha_n a)}{\alpha_n^2\left(\frac{\alpha_n}{\tanh \alpha_n l} + H\right) J_0^2(\alpha_n b)}\right]}{1 - \frac{4H}{b^2}\sum_{n=1}^{\infty}\frac{J_1^2(\alpha_n a)}{\alpha_n^2\left(\frac{\alpha_n}{\tanh \alpha_n l} + H\right) J_0^2(\alpha_n b)}} \qquad \text{(A-23)}$$

The temperature distribution in the copper $T_c(r)$ can now be determined by combining Equations (A-13), (A-22), and (A-23).

These equations can be simplified for application to the experiments described in this paper, since the experimental value of H was fairly small and the value of l was quite large. Under these conditions Equation (A-23) becomes

$$\frac{dT_c}{dr}(a) = \frac{S}{2a}(b^2 - a^2) \qquad \text{(A-24)}$$

and Equation (A-22) is simplified to

$$A_n = \frac{-2 S a J_1(\alpha_n a)}{\alpha_n^3 b^2 J_0^2(\alpha_n b)} \qquad \text{(A-25)}$$

Substituting Equation (A-25) into Equation (A-13) and noting that $\tanh \alpha_n l = 1$ for large values of l, we get finally

$$\frac{T_c(r)}{S} = \frac{1}{4}\left(a^2 - r^2 + 2b^2 \ln \frac{r}{a}\right) + \frac{2aH}{b^2}\sum_{n=1}^{\infty}\frac{J_1(\alpha_n a)}{\alpha_n^4 J_0^2(\alpha_n b)}\left[J_0(\alpha_n r) - J_0(\alpha_n a)\right] \qquad \text{(A-26)}$$

Experimental Design "B"

Differential Equation (A-9) describing the temperature distribution in the copper can be rewritten as

$$\frac{d}{dr}\left[r\frac{dT_c}{dr}\right] = -r\left[S + H\frac{\partial T_w}{\partial z}\bigg|_{z=0}\right] \qquad \begin{matrix} a < r < b \\ z = 0 \end{matrix} \qquad \text{(A-27)}$$

The boundary conditions appropriate to experimental design "B" are

$$\text{B.C.1}\ \frac{dT_c}{dr} = 0 \quad r = b \qquad \text{(A-28)}$$

$$\text{B.C.2}\ \frac{dT_c}{dr} = 0 \quad r = a \qquad \text{(A-29)}$$

Before proceeding, it should be noted that it is quite reasonable to expect the temperature profile at $z = 0$ to change abruptly between a point at slightly less than 'a' and a point at $r = a$, since there is no radial heat flow across the copper surface at $r = a$. Although this abrupt change is easily represented mathematically as a discontinuity in temperature at $r = a$, a solution for the temperature distribution in the copper can be obtained only if the size of the discontinuity is specified or if a sufficient restriction is placed on the shape of the temperature profile in the copper. In this problem the temperature of the copper in the interval is taken as constant. Proceeding, then, toward evaluating this constant, one can integrate Equation (A-27) with respect to r to get

$$\int_a^b r\frac{\partial T_w}{\partial z}(r, 0)\, dr = -\frac{S}{2H}(b^2 - a^2) \qquad \text{(A-30)}$$

after applying boundary conditions (1) and (2). Differentiating Equation (A-2) with respect to z and evaluating the result at $z = 0$ one yields

$$\frac{\partial T_w}{\partial z}(r, 0) = \frac{2aT_c}{b^2}\sum_{n=1}^{\infty}\frac{J_0(\alpha_n r) J_1(\alpha_n a)}{J_0^2(\alpha_n b)}\tanh \alpha_n l \qquad \text{(A-31)}$$

since $T_c(r) = \text{constant} = T_c$. Substituting Equation (A-31) into Equation (A-30) and solving for T_c, we get

$$T_c = \frac{S b^2 (b^2 - a^2)}{4H a^2 \sum_{n=1}^{\infty}\frac{1}{\alpha_n}\left[\frac{J_1(\alpha_n a)}{J_0(\alpha_n b)}\right]^2 \tanh \alpha_n l} \qquad \text{(A-32)}$$

For large values of l Equation (A-32) reduces to

$$T_c = \frac{S b^2 (b^2 - a^2)}{4H a^2 \sum_{n=1}^{\infty}\frac{1}{\alpha_n}\left[\frac{J_1(\alpha_n a)}{J_0(\alpha_n b)}\right]^2} \qquad \text{(A-33)}$$

Manuscript received March 4, 1965; revision received June 7, 1965; paper accepted June 8, 1965.